Quantum dot sensitized solar cells: Effect of nanocrystal size on the efficiency

Neetu Singh[1,2], R.M.Mehra[3]*, Avinashi Kapoor[1], T.Soga[4]

[1]Department of Electronic Science, University of Delhi South Campus, (NewDelhi)-110 021, (INDIA)
[2]Department of Electronics, Keshav Mahavidyalaya, University of Delhi, Delhi- 110 034, (INDIA)
[3]School of Engineering and Technology, Sharda University, Greater Noida-201 306, (INDIA)
[4]Graduate School of Engineering, Nagoya Institute of Technology, Gokiso-cho, Showa-ku, Nagoya 466-8555, (JAPAN)

ABSTRACT

Bandgap of the CdSe nanocrystals was tailored using low temperature synthesis and these nanocyrstals were used to fabricate ZnO based Quantum Dot Sensitized Solar Cell (QDSSC). CdSe nanocrystal size varied from 0.85 to 2.25 nm with increase in synthesis temperature from 225 to 255°C. Bandgap of CdSe nanocrystals decreased from 3.50 to 1.97 eV with increase in size from 0.85 to 2.25 nm, resulting in the absorbance of a broader spectrum of visible light in the range 350 to 700 nm. QDSSCs were fabricated by using individual nanocrystals of different size and a blend of all the nanocrystals. As the size of the nanocrystal increased from 0.85 to 2.25 nm, efficiency of QDSSC was found to decrease from 2.06 to 0.25 %. The efficiency of colloidal QDSSC cell was obtained to be 3.6 % at AM 1.5.
© 2014 Trade Science Inc. - INDIA

INTRODUCTION

Semiconductor nanocrystals of narrow bandgap materials such as CdSe, CdS, PbS and InAs have been the subject of considerable interest due to their potential to replace the sensitizer dyes in Dye Sensitized Solar Cells (DSSCs)[1-5]. QDSSCs have the possibility of boosting the power conversion efficiency beyond the traditional Schokley and Queisser limit of 31% for Si based solar cells[6]. QDSSCs make use of quantum dot nanocrystals as sensitizers in the front wide bandgap electrode. DSSCs have exhibited a maximum power conversion efficiency of 11.1 % and a good long term stability but in order to outwit the traditional Schokley

and Queisser limit of 31% for Si based solar cells, further research needs to be focused to increase the efficiency of DSSCs[7]. For maximum power conversion efficiency in DSSCs, the dyes used as sensitizers should highly absorb in the entire visible spectrum. This is possible only when several dyes absorbing different wavelengths of the visible region are used simultaneously in colloidal form. QDSSCs make use of quantum dot nanocrystals instead of dyes because the size quantization property of quantum dot nanocrystals allows one to modulate bandgap offsets and in turn to tune the visible response. The smaller sized nanocrystal has larger bandgap and vica-versa. The main advantage with quantum dot nanocrystals is that, because of the high

Full Paper

level of control possible over the size of the nanocrystals produced, it is possible to have very precise control over the conductive properties of the material[8]. Thus quantum dot nanocrystals of the same material, but with varying sizes, can absorb as well as emit light of different wavelengths. Compared to traditional dyes, quantum dot nanocrystals have broader and tuneable absorption wavelength, high extinction coefficient, more resistant to chemical and metabolic degradation, higher photobleaching threshold, and high quantum yield[9]. Furthermore, these nanocrystals utilize hot electrons and generate multiple charge carriers with a single photon[10] This phenomenon is called Multiple Exciton Generation (MEG). As a result, they have superior transport and optical properties, and are being researched for use in solar cells, diode lasers, amplifiers, and biological sensors etc. Due to MEG quantum dot nanocrystals are able to increase the efficiency and reduce the cost of today's typical Si photovoltaic cells[11,12]. This compares favorably to today's photovoltaic cells which can only manage one exciton per high energy photon, with high kinetic energy carriers losing their energy as heat. QDSSCs are cheaper to manufacture, as they can be made using simple laboratory techniques[13].

Three methods of assembling quantum dot nanocrystals into mesoporous TiO_2/ZnO films have been reported so far: in situ growth of nanocrystals on TiO_2/ZnO surface using Chemical Bath Deposition (CBD), deposition of presynthesized colloidal nanocrystals by direct adsorption and deposition of presynthesized colloidal nanocrystals by using bifunctional linking molecule such as Mercapto Propionic Acid (MPA)[11]. Research is been going on the fabrication of QDSSCs using all three methods. But growth of quantum dot nanocrystals using CBD and then fabricating QDSSC on this layer has been rigorously studied. Direct adsorption of nanocrystals on TiO_2/ZnO surface results in poor linking of the nanocrystals with nanoporous structure of TiO_2/ZnO. So, a suitable bidirectional linking molecule is used whose one end is attached to the nanocrystals and other end is attached to TiO_2/ZnO nanoporous structure. Use of suitable linking molecule enhances the power conversion efficiency because of the proper linking of nanocrystals with TiO_2/ZnO network. Now a days research is more focused on ZnO as front electrode in QDSSC because of its very nature of being self activated n-type semiconductor, large exciton binding energy of 60 meV, more stability to high energy radiation and wet chemical etching[14]. Luan et. al have also reported efficiency of ~ 1% in a ZnO nanorod/CdS/CdSe based QDSSC[15] while Chen et. al have used CdS and CdSe as a co-sensitized in QDDSC with ZnO nanowire, However maximum efficiency is reported 1.4%[16].

This paper reports a simple chemical route to synthesize of CdSe nanocrystals for preparation of QDSSCs. The effect of synthesis temperature on structural and optical properties of the nanocrystals is investigated. Effect of nanocrystal size on the QDSSC performance is also investigated. An empirical relation has been developed to correlate the efficiency of the cells with the size of CdSe nanocrystals.

EXPERIMENTAL

Synthesis of CdSe nanocrystals

CdSe nanocrystals were prepared by low temperature synthesis. For Se source, 30 mg of Selenium (Se) and 5 ml octadecene were added in a flask and stirred on a magnetic stirrer with 80°C temperature. 0.4 ml Tri-Octyl Phosphine (TOP) was added to the above mixture. The solution was stirred while giving the temperature at the same time to completely dissolve the selenium. When Se was dissolved completely, the solution was cooled to room temperature. This solution may be prepared ahead of time, and has enough Se precursors for several preparations, and can be stored in a sealed container for at least several months. To prepare CdSe nanocrystals, 13 mg of CdO was mixed in 10 ml octadecene in a flask. To the same flask, 0.6 mL oleic acid was added. Flask was swirled to mix the liquids. This solution was heated till the temperature reached 225°C. 1mL of Se solution was then added to this CdO solution. The control of the size of the nanocrystals was achieved simply by controlling synthesis temperature[18]. The temperature was increased gradually (225-255°C) as the reaction progressed. CdSe nanocrystals were then removed at frequent intervals with help of micropipette as the CdSe particles grew in size by noticing the change in the color of the solution. As the reaction progressed, the solution was

observed to change its color from green to red. XRD measurements of CdSe nanocrystals were carried out using Bruker AXS – D8 discover diffractometer having CuK$_\alpha$ incident beam ($\lambda = 1.54$Å). Structural properties of CdSe nanocrystals were observed by using TECNAI G^2 T30, u-TWIN TEM.

Preparation of ZnO electrode

Slurry of ZnO nanoparticles with polyethylene glycol (PEG $_{20,000}$) in Di-ionized (DI) water was used to prepare ZnO electrode using Doctor-blade technique. Bare ZnO electrode was first prepared and sintered at 450$^{R''}$C. The details of preparing ZnO electrode without and with nanocrystals are reported elsewhere[17]. Absorbance of CdSe nanocrystals and CdSe nanocrystals adsorbed ZnO electrode in the visible region was measured using Shimadzu solidspec-3700 UV-VIS-NIR spectrophotometer.

Fabrication of quantum dot sensitized solar cell

QDSSCs were fabricated by using individual QDs of different size and a blend of all the nanocrystals. The blend of nanocrystals was formed by ultrasonication of all the nanocrystals for 2 h. QDSSC fabrication technique has been reported in detail elsewhere[19] of the ZnO electrode changed to dark yellow after nanocrystal adsorption. I-V characteristic of the cell was measured using computerized digital 2400 Keithley source meter and a M-91190 Newport class-A solar simulator. The measurement was made at 1 sun illumination (100 mW/cm^2, AM 1.5). The active electrode area was typically 1 cm^2.

RESULTS AND DISCUSSION

CdSe nanocrystals

The XRD pattern of CdSe nanocrystals is shown in Figure 1. The wurtzite crystalline structure of CdSe corresponding to (002) plane at 25° is observed in all spectra of nanocrystals[20]. The extremely broad diffraction peak of XRD pattern indicates about the extremely small size of the nanocrystals. The single peak in (002) plane indicates the preferential growth of crystallites in this particular plane showing the singly crystalline nature of nanocrystals. No additional impurity peaks are found in XRD spectra. Full Width at Half

Maximum (FWHM) is found to decrease as synthesis temperature increases showing that nanocrystal size increases with increase in synthesis temperature. Debye-Scherrer's formula was used to calculate the nanocrystal size (D)[20].

$$D = \frac{K\lambda}{\beta\cos\theta} \qquad (1)$$

Where, K is the particle shape factor which depends on the shape of the particles and its value is 0.94, β is FWHM of the selected diffraction peak corresponding to (002) plane and θ is the Bragg angle obtained from 2θ value corresponding to the same plane.
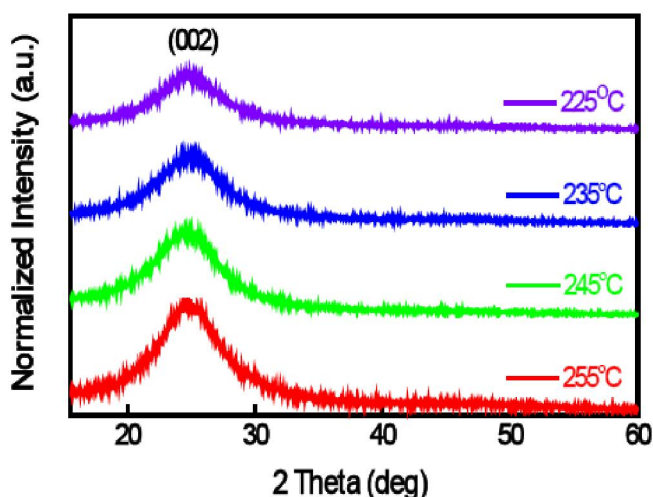

Figure 1 : Effect of synthesis temperature on XRD pattern of CdSe nanocrystals
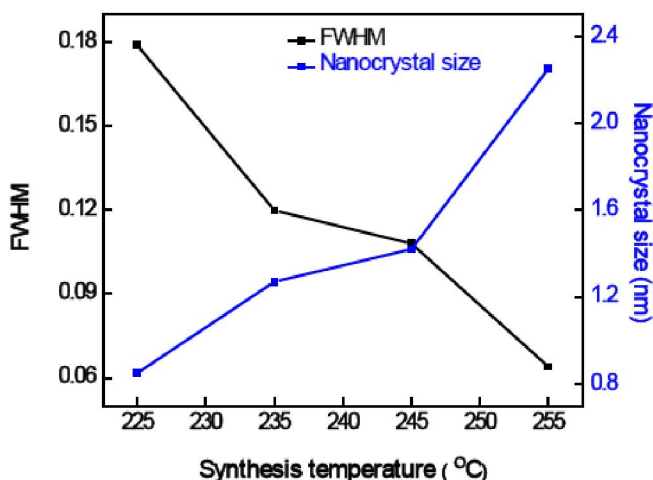

Figure 2 : Variation in FWHM and CdSe nanocrystal size as a function of synthesis temperature

Figure 2 shows the effect of synthesis temperature on FWHM and nanocrystal size. The size of the nanocrystals increases from 0.85 to 2.25 nm with in-

Full Paper

crease in synthesis temperature may be due to high reaction rate or the expansion of capping agent polymer matrix because of increased synthesis temperature.

TEM analysis was further carried out to investigate more about structural analysis CdSe. Figure 3 shows the TEM images of CdSe nanocrystals at different synthesis temperature. Size of CdSe nanocrystals is varying from 0.85 to 2.25 nm with increase in the synthesis temperature from 225 to 255°C. TEM images are arranged in increasing order of synthesis temperature wich also support the formation of CdSe quantum dot nanocrystals. Size of CdSe nanocrystals as calculated by XRD matches well with the TEM results.
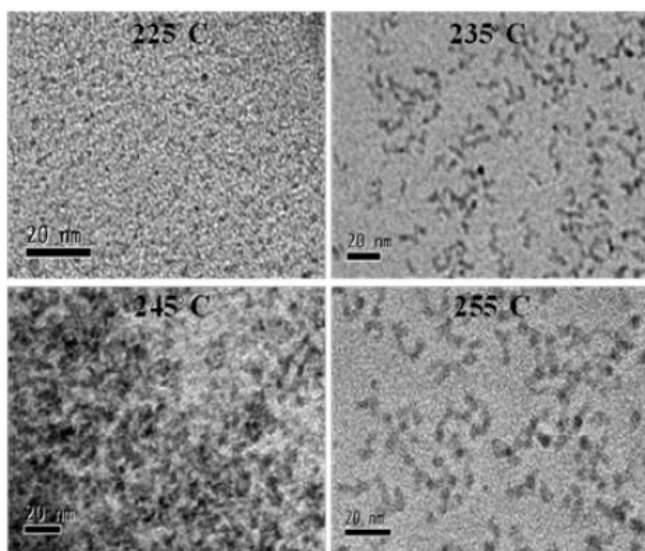

Figure 3 : TEM images of CdSe nanocrystals with different synthesis temperature

The optical absorption spectra of the CdSe nanocrystals are shown in Figure 4 (a). The bandgap of bulk CdSe is 1.74 eV and the absorption peak is observed at ~ 715 nm. The absorption peak of CdSe nanocrystals is red shifted with increase in synthesis temperature due to increase in nanocrystal size. The inset of Figure 4 (a) shows the change in color of synthesized nanocrystals. Bandgap (E_g) of nanocrystals was calculated using Tauc's plot method (Eq. 2) is given by[17].

$$\alpha h\upsilon = A\,(h\upsilon - E_g)^n \tag{2}$$

Where, α is the absorption coefficient, $h\upsilon$ is the photon energy, A is the constant, E_g is the bandgap. The value of n is ½ or 2 depending upon whether the transition from valence band to conduction band is direct or indi-

rect. The value is ½ in case of direct transition and 2 in case of indirect transition. Since CdSe is a direct bandgap semiconductor, the value of n is ½ in the present case. The Tauc's plot is shown in Figure 4 (b). Intersection of the slope of $(\alpha h\upsilon)^2$ Vs $h\upsilon$ curve provides bandgap. The bandgap is found to vary from 1.97 to 3.50 eV as the synthesis temperature decreases. The Bohr radius of exciton for CdSe is 5.6 nm[21,22], The CdSe nanocrystal size is less than the exciton Bohr radius indicating a strong quantum confinement.

ZnO electrode

The surface morphologies of bare ZnO electrode and CdSe sensitized ZnO electrode were studied using SEM. SEM images show that bare ZnO electrode has porous structure which is necessary for CdSe adsorption (Figure 5). After adsorption of CdSe nanocrystals on the mesoporous ZnO electrode, the pores of ZnO are filled by the nanocrystals. SEM image confirms that the nanocrystals sit in the porous structure of ZnO electrode. It can be see that after nanocrystal adsorption, the ZnO nanoporous structure is partially blocked so as to provide the necessary pathway for the movement of charge carriers as well as electrolyte redox couple ions.

Absorbance spectra of ZnO electrode before and after CdSe sensitization is shown in Figure 6. Bare ZnO electrode absorbed light in only UV region of less than 400 nm, due to its wide bandgap (3.37 eV for bulk). Absorbance increased in the visible region and covered almost entire visible spectrum from 350 to 700 nm with sensitization of ZnO electrode with CdSe nanocrystals. Size quantization effect red shifted the absorption edge indicating the adsorption of all CdSe nanocrystals having different absorption wavelength, thereby covering the entire visible spectrum.

Quantum dot sensitized solar cell

I-V characteristic of the QDSSC is shown in Figure 7. The power conversion efficiency (η) and fill factor (FF) were evaluated using following relations (Eq. 3 & 4)

$$\eta = \frac{I_m \times V_m}{P_{in}} \times 100 \; (\%) \tag{3}$$

$$FF = \frac{I_m \times V_m}{I_{sc} \times V_{oc}} \tag{4}$$
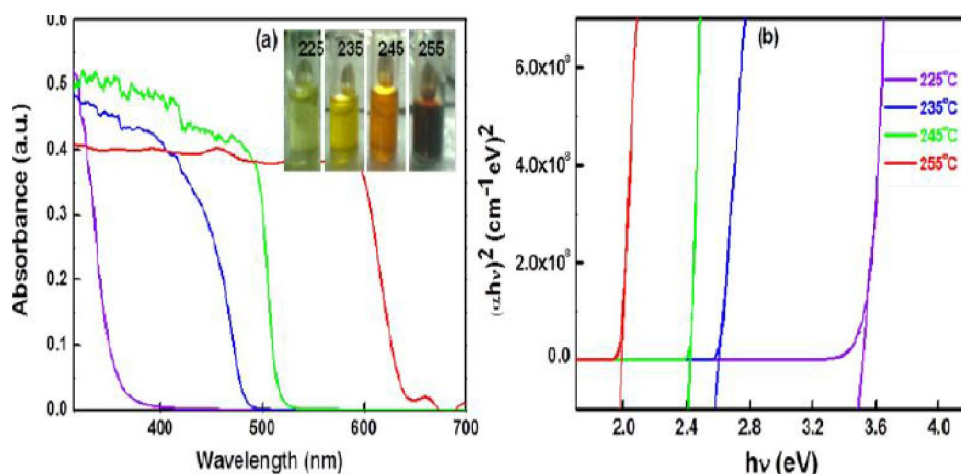
Figure 4 : (a) Absorption spectra (inset - CdSe nanocrystals in increasing order of size) and (b) Tauc's plots of CdSe nanocrystals
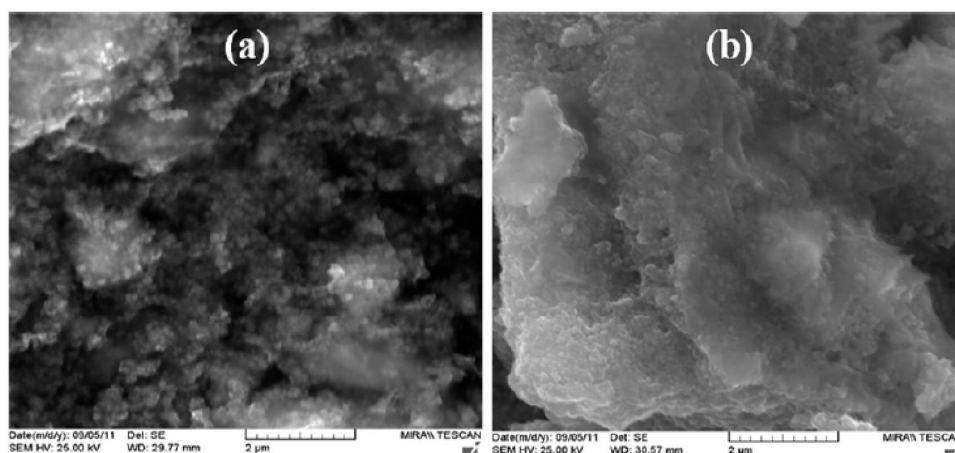

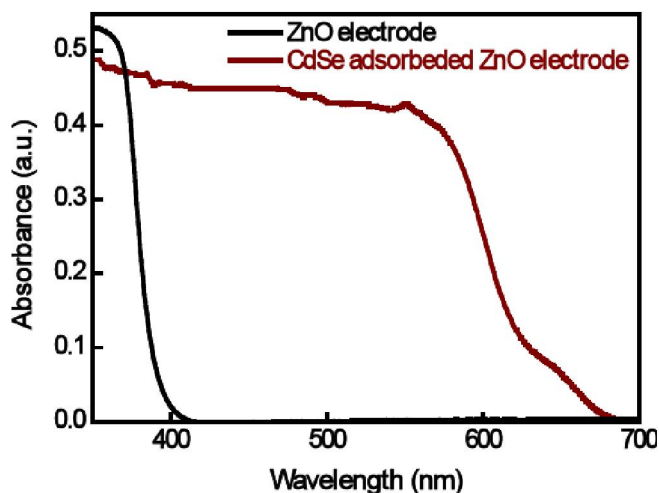**Figure 5 : SEM images of (a) bare ZnO electrode and (b) CdSe adsorbed ZnO electrode**

Figure 6 : Absorbance graph of ZnO electrode without and with CdSe adsorption

Where, I_{sc} is the short-circuit photocurrent, V_{oc} is the open circuit photo voltage and P_{in} is the incident light power. I_m and V_m are the current and voltage at the

TABLE 1 : Effect of nanocrystal size on various parameters of QDSSC

Nanocrystal size (nm)	I_{sc} (mA)	V_{oc} (V)	I_m (mA)	V_m (V)	FF	η (%)
0.85	5	0.71	4.4	0.47	0.6	2.06
1.2	3.7	0.66	4.3	0.44	0.8	1.9
1.34	2.19	0.58	1.8	0.37	0.52	0.66
2.25	1.17	0.38	0.88	0.28	0.6	0.25
Colloidal QDSSC	10.5	0.78	7.4	0.48	0.5	3.6

maximum power point (P_m) respectively. The values of I_{sc}, V_{oc}, P_m, FF and η for QDSSCs fabricated using different sized nanocrystals are given in TABLE 1.

The efficiency of the QDSSC is found to increase with decrease in the size of the nanocrystals. This is because the efficiency is directly dependent on number of photo-generated charge carriers which in turn depend on the charge transfer rate between nanocrystals
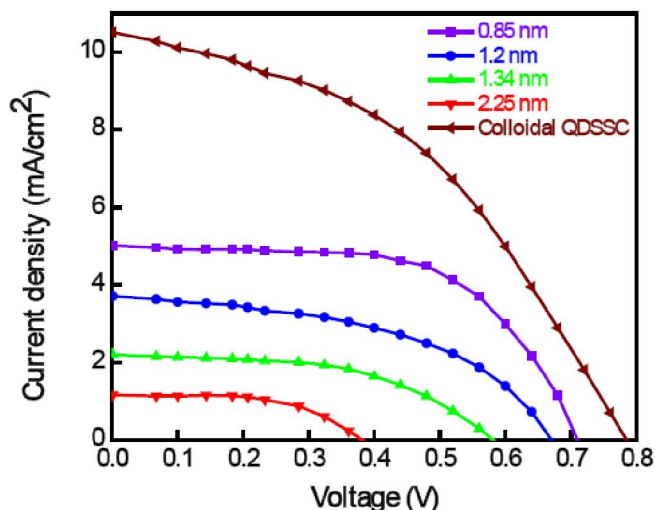
Full Paper

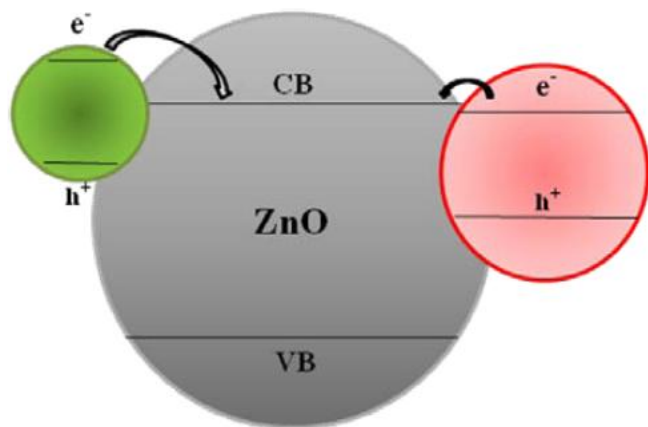**Figure 7 : I-V characteristics of CdSe nanocrystals sensitized QDSSCs**

Figure 8 : Simple charge injection model

and ZnO. Larger nanocrystals may absorb more photons, but may not transfer the generated charges efficiently to the acceptor material. The charge injection rate is dependent on the difference between the nanocrystal excited state and conduction band of ZnO. Since larger sized nanocrystal has smaller bandgap as compared to the smaller sized nanocrystal which has larger bandgap (Figure 8), the rate of charge injection is higher in case of smaller sized nanocrystals. Therefore the I_{sc} and hence efficiency is improved as the size of the nanocrystal decreases. The highest power conversion efficiency of 3.6 % has been obtained in case of blended nanocrystal QDSSC. This is attributed to the efficient light harvesting and charge collection resulting from enhanced light absorption due to the larger distribution in size of nanocrystals. When all the nanocrystals having absorption maximum edges in the

entire visible spectrum are mixed together, then the absorption of the photons by the nanocrystals is maximized and the result is an overall improved efficiency.

An empirical model (Eq. 5) is also obtained by fitting the experimental data, to see the effect of nanocrystal size on the efficiency of the cells. Where, $A_1 = 2.05$, $A_2 = 0.33$, $D_0 = 1.27$, $dx = 0.03$.

$$\eta = A_2 + \frac{(A_1 - A_2)}{(1 + \exp((D - D_0)/dx))} \qquad (5)$$

The variation in efficiency with nanocrystal size using the above relationship is shown in Figure 9. For better understanding, Figure 9 is divided into three regions – region-I, region-II and region-III. It can be seen that rate of change of efficiency is highest in region-II. This may be explained by the charge injection model (Figure 8). As we know that the major mechanism of charge separation in a QDSSC is the energy level position of the whole system. The excited state of the nanocrystals should lie above the conduction band edge of the ZnO and ground state of the nanocrystals should lie below the chemical potential of the electrolyte, for efficient charge injection and separation. So the rate of charge injection in case of smaller sized nanocrystals is higher because of high energetic driving force which injects the electrons into the conduction band of ZnO due to which the rate of efficiency increase is more in region-II as compared to region-III. But, the rate of efficiency change is small in region-I although it contains more small nanocrystals. This may be due to the smaller density of the crystals or not good compatibility
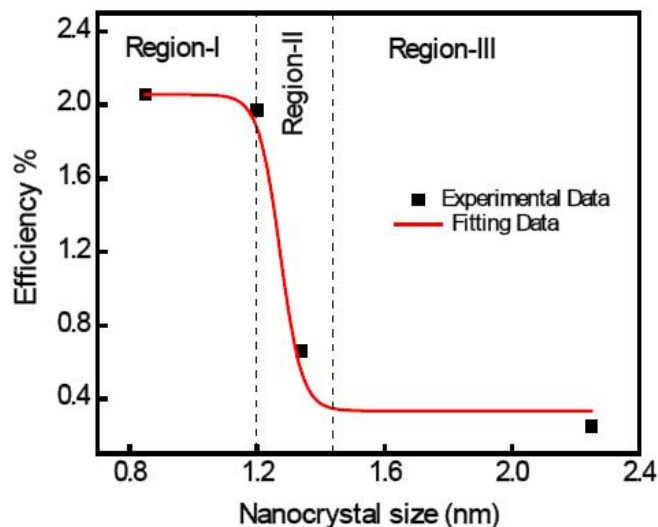

Figure 9 : Effect of nanocrystal size on efficiency of QDSSC

Full Paper

between nanocrystal size and ZnO pore size.

CONCLUSION

CdSe nanocrystals of size varying in the entire visible spectrum offer new ways to design QDSSCs with a broader absorption range. So, an easy, cost effective and size tunable synthesis of the CdSe nanocrystals was employed to tune the bandgap in the range 400 to 700 nm. Synthesis temperature was shown to have a strong effect on the size of nanocrystals and hence absorption onset. The deposition of such QD nanocrystals covering the entire visible spectrum, into ZnO film forms maximizes the light harvesting capability of QDSSCs. As the size of nanocrystals increased from 0.85 to 2.25, the efficiency of QDSSC was found to decrease from 2.06 to 0.25 %. The QDSSC with smallest size nanocrystals have maximum efficiency of 2.06 % due to faster charge transfer rate because of high energetic driving force. The efficiency of colloidal QDSSC was obtained 3.6 % due to better synergy for harvesting incident photons of a broader spectrum of visible light. The fabrication of colloidal QDSSC paves the way for improving the efficiency of solar cells.

ACKNOWLEDGEMENTS

REFERENCES

[1] M.Gratzel, J.Photochem; Photobiol, **C4**, 145 **(2003)**.
[2] O.Niitsoo, S.K.Sarkar, C.Pejoux, S.Riihle, D.Cahen, G. Hodes; J. Photochem. Photobiol, **A181**, 306 **(2006)**.
[3] T.Toyoda, J.Sato, Q. Shen; Rev. Sci. Instrum., **74**, 297 **(2003)**.
[4] Q.Shen, T.Toyoda; Jap. J. Appl. Phys., **43**, 2946 **(2004)**.
[5] Robel, V.Subramanian, M.Kuno, P.V.Kamat; J. Am. Chem. Soc., **128**, 2385 **(2006)**.
[6] W.Schokley, H.J.Queisser; J. Appl. Phys., **32**, 510 **(1961)**.
[7] Y.Chiba, A.Islam, Y.Watanabe, R.Komiya, N.Koide, L.Han; Jpn. J. Appl. Phys., **45**, L638 **(2006)**.
[8] P.V.Kamat; J. Phys. Chem., **C112**, 18737 **(2008)**.
[9] B.Suo, X.Su, J.Wu, D.Chen, A.Wang, Z.Guo; Mater. Chem. Phys., **119**, 237 **(2010)**.
[10] Y.L.Lee, B.M.Huang, H.T.Chien; Chem. Mater., **20**, 6903 **(2008)**.
[11] J.Chen, J.L.Song, X.W.Sun, W.Q.Deng, C.Y.Jiang, W.Lei, J.H.Huang, R.S.Liu; Appl. Phys. Lett., **94**,153115 **(2009)**.
[12] J.B.Sambur, T.Novet, B.A.Parkinson; Science, **330**, 63 **(2010)**.
[13] D.R.Baker, P.V.Kamat; Adv. Funct. Mater., **19**, 805 **(2009)**.
[14] V.Kumar, R.G.Singh, L.P.Purohit, R.M.Mehra; J. Mater. Sci. Technol., **27** 481 **(2011)**.
[15] C.Luan, A.Vaneski, A.S.Susha, X.Xu, H.E.Wang, X.Chen, J.Xu, W.Zhang, C.Lee, A.L.Rogach, J.A.Zapien; Nanoscale. Res. Lett., **6**, 340 **(2011)**.
[16] J.Chen, J.Wu, W.Lei, J.L.Song, W.Q.Deng, X.W.Sun; Appl. Surf. Sci., **256**, 7438 **(2010)**.
[17] D.W.Ayele, H.Chen, W.Su, C.Pan, L.Chen, H.Chou, J.Cheng, B.Hwang, J.Lee; Chem. Eur. **J17**, 5737 **(2011)**.
[18] N.Singh, R.M.Mehra, A.Kapoor, T.Soga; J. Renew. and Sustain. Ener., **4**, 013110 **(2012)**.
[19] S.Neeleshwar, C.L.Chen, C.B.Tsai, Y.Y.Chen; Phys. Rev., **B71**, 201307 **(2005)**.
[20] E Lifshitz, I.Dag, I.Litvin, G.Hodes, S.Gorer, R.Reisfeld, M.Zelner, H.Minti; Chem. Phys. Lett., **288**, 188 **(1998)**.
[21] S.S.Narayanan, S.K.Pal; J.Phys. Chem., **B110**, 24403 **(2006)**.